

Temperature measurements using real-time holographic interferometry in a tank fire – influence of species composition

Markus Gawłowski, Kerry Kelly*, Peter Sudhoff, Iris Vela, Axel Schönbacher

* Institute for Combustion & Energy Studies, University of Utah, Salt Lake City, USA

University of Duisburg-Essen, Germany www.uni-due.de/tech1chem markus.gawłowski@uni-due.de

32nd International Symposium on Combustion
McGill University, Montreal, Canada, August 3-8 2008

1 Introduction

Non-premixed pool and tank fires can occur during the transportation or storage of hazardous materials, e.g. liquid hydrocarbon fuels, and could cause large accidents. Therefore, a first step is to study laboratory-scale tank fires.

Temperature measurements of laboratory-scale fires using holographic interferometry allow the calculation of numerous variables of interest including heat transfer to the surroundings or impinging objects. When flame temperatures are determined from interferograms, the concentration of species with a large effect on specific refraction should be known.

For a small-scale tank fire the three different flow regions are presented in Fig. 1.

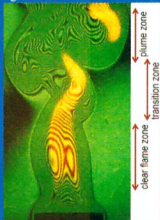
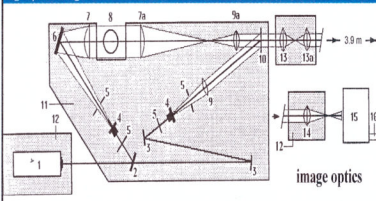


Fig. 1: Interferogram of an n-hexane tank fire (d=5cm) superimposed with the visible fire field.

2 Experimental

Temperature fields were measured using real-time holographic interferometry (HI) of 5-cm n-hexane fires above a cylindrical steel tank. The hexane level was held at a constant level of 2 mm below the tank rim. The mass burning rate of n-hexane was $\dot{m} = 0.024 \text{ kg/(m}^2\text{s)}$, and the volume flow rate of n-hexane was adjusted to $\dot{V} = 0.06 \text{ ml/s}$ at a constant temperature of $T = 293 \text{ K}$. The holographic interferogram and the visible flame field were recorded simultaneously by a high-speed camera (see Fig. 2). A low-temperature gas chromatograph provided concentrations of the major stable species with a concentration of greater 0.05 Vol.%, e.g. C_6H_{14} , O_2 , N_2 , H_2O , CO_2 , CO , C_2H_4 and H_2 .



- 1.) 2 W-cw-Argon laser
- 2.) beam splitter
- 3.) mirror
- 4.) beam expanding
- 5.) shutter
- 6.) 22 cm plate mirror
- 7.) 25 cm lens (plan convex)
- 8.) testroom for phase object
- 9., 9a) 7.8 cm achromat, $f = 31 \text{ cm}$
- 10.) hologram
- 11.) granite plate (3 m x 1.3 m)
- 12.) concrete finished products
- 13., 13a) 7.8 cm achromat, $f = 16 \text{ cm}$
- 14.) 7.8 cm achromat, $f = 31 \text{ cm}$
- 15.) high speed camera (Hycam)
- 16.) microscope ocular

Fig. 2: High-speed holographic real-time interferometer (Mach-Zehnder) with a 25 cm beam expansion described in [1] and the image optics

4 Conclusions and Future Work

Holographic interferometry is a useful method to obtain temperature fields from small-scale tank fires however temperatures measured using HI require the local concentrations of the species in non-premixed flames. The results show that with increasing height the effect of species concentration on fire temperatures decreases and the turbulence effect increases resulting in smaller gradients e.g. of

3 Results

3.1 Physical interpretation of the interference fringe field

$$S(x, y, t) \lambda = \int_{-z(y)}^{+z(y)} (n_m(x, y, z, t) - n_a) dz$$

$$n_m(r, x, t) - n_a = -\frac{\lambda}{\pi} \int_r^R \frac{\partial S(x, y, t)}{\sqrt{y^2 - r^2}} dy \quad (\text{Abel transformation})$$

$$\rho_m(r, x, t) = \frac{2}{3} (n_m(r, x, t) - 1) \frac{\sum \gamma_i(r, x, t)}{\sum \gamma_i(r, x, t) N_{i,0}} \quad (\text{Gladstone-Dale})$$

$$T_m(r, x, t) = \frac{1}{\rho_m(r, x, t)} \frac{\sum \gamma_i(r, x, t) \rho_{i,1,0}}{\sum \gamma_i(r, x, t)} T_0$$

$S(x, y, t)$	Field of the interference fringe order	n_m	Refractive index of flame-gas mixture
n_a	Refractive index of ambient air	λ	Laser wavelength ($\lambda = 514.5 \text{ nm}$)
r	Radial coordinate	R	Radius of the flame including the thermal boundary layer
ρ_m	Density of flame-gas mixture	γ	Mass fraction of stable species i
$N_{i,0}$	Specific standard refraction of species i	T_0	Temperature at standard conditions ($T = 273 \text{ K}$)
N_m	Specific refraction of flame-gas mixture	T_m	Temperature of flame-gas mixture

3.2 Radial profiles of the interference fringe order (Fig. 3), specific refraction (Fig. 4), density (Fig. 5) and temperature (Fig. 6) at different heights x above the tank rim

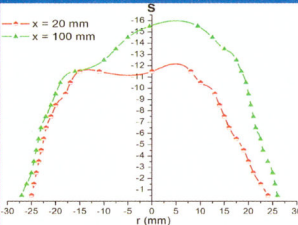


Fig. 3: Radial $S(r, x, t)$ profiles

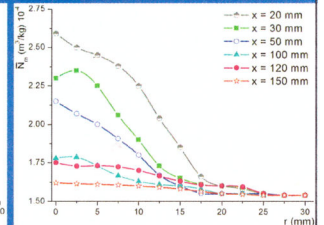


Fig. 4: Radial $N_m(r, x)$ profiles

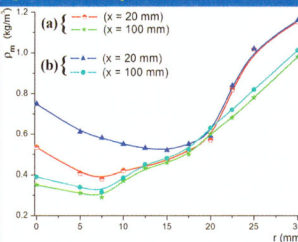


Fig. 5: Radial $\rho_m(r, x, t)$ profiles with (a) $N_m(r, x)$ profiles (b) uniform composition of $N_m(r, x) = N_{m,0}$

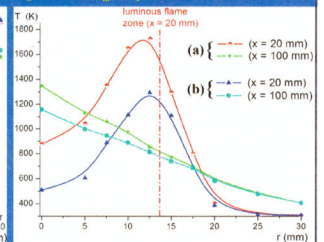


Fig. 6: Radial $T(r, x, t)$ profiles with (a) $N_m(r, x)$ profiles (b) uniform composition of $N_m(r, x) = N_{m,0}$

temperatures. Future work will focus on temperature fields of tank fires with different hydrocarbon fuels and diameters ($1 \text{ cm} < d < 10 \text{ cm}$). The results will be used for validation of CFD simulated interferograms.

Literature

- [1] A. Schönbacher, B. Arnold, V. Banhardt, V. Bieller, H. Kasper, M. Kaufmann, R. Lucas, N. Schieb, *Simultaneous observation of organized density structures and the visible field in pool fires*, Proc. Combust. Inst. 21 (1986) 83-92